N
m 1X

AEROSPACE REPORT NO.
ATR-73(8102)-4
CR 114510
AVAILABLE TO PUBLIC

SOLAR FLARE FORECASTS BASED ON mm-WAVELENGTH MEASUREMENTS

Prepared by K. P. WHITE, III
Space Physics Laboratory

72 OCT 25

Prepared for NASA AMES RESEARCH CENTER
Moffett Field, California

Contract No. NAS2-6654

Laboratory Operations
THE AEROSPACE CORPORATION

(NASA-CR-114510) SOLAR FLARE FORECASTS BASED ON mm-WAVELENGTH MEASUREMENTS K.P. White, III (Aerospace Corp., El Segundo, Calif.) 25 Oct. 1972 40 p CSCL 03B
N73-11815
Unclas
G3/29 46892

Aerospace Report No.
ATR-73(8102)-4

SOLAR FLARE FORECASTS BASED ON mm-WAVELENGTH MEASUREMENTS

Prepared by
K. P. White, III
Space Physics Laboratory

72 OCT 25

Laboratory Operations
THE AEROSPACE CORPORATION
El Segundo, California

Contract No. NAS2-6654

Prepared for
NASA AMES RESEARCH CENTER
Moffett Field, California

Report No.
ATR-73(8102)-4

SOLAR FLARE FORECASTS BASED ON
mm-WAVELENGTH MEASUREMENTS

Prepared

K. P. White, III

K. P. White, III

Approved

E. B. Mayfield

E. B. Mayfield, Head
Solar Physics Department

G. A. Paulikas

G. A. Paulikas, Director
Space Physics Laboratory

ABSTRACT

Solar radio temperature contour maps made at The Aerospace Corporation at a wavelength of 3.3 mm are analyzed to develop a method of forecasting solar flares of classes 1N and 1B. Fundamental to the ensuing analysis is the demonstration that most of the radio sources associated with the sunspot-plage systems are not spatially resolved by the radio telescope and, hence, only the peak temperature enhancements due to these local radio sources are employed in the study. Evidence is presented indicating that flare-prone plage regions, which belong to recurrent families of flare-productive regions, exhibit a relationship between flare production and radio temperature characteristics considerably unlike that exhibited by virgin plage regions, which do not have such a history of flare activity. Most importantly, the results are interpreted by means of graphs which permit the inference of class 1B or 1N flare probabilities based on the peak temperature enhancements measured at 3.3 mm. In particular, the forecast obtained is the probability that a given flare-prone plage region will produce a class 1B or 1N flare (two quoted probabilities) during the period of its disk transit.

CONTENTS

FIGURES

TABLES

I. INTRODUCTION

This report is in response to Task IV of NASA contract NAS 2-6654 "Solar Flare Predictions and Warning." The purpose of this task is to perform an analysis of solar radio temperature contour maps made at a wavelength of 3.3 mm in order to determine the feasibility of forecasting solar flares of optical class 1. The report consists of an explanation of the rationale employed, a critical review of the data obtained, the analysis of these data and, finally, the consequences these results have in the application of the method to accurate forecasting of class 1 solar flares.

The data to be input to the forecasting method developed in this report are obtained from daily solar radio maps made using the 15-ft radio telescope of the Aerospace Corporation, which is described by Mayfield et al. (1970) and in more detail in references cited therein. The analytical scheme employed in the interpretation of the radio maps is that established by Mayfield et al. (1970); a very brief recapitulation of their method and conclusions is appropriate at this point.

The analysis of the radio maps begins with selection of an inactive region on the solar disk, which serves as a normalization point for temperature readings across the whole solar disk. Contours are then drawn through equal temperature readings in increments of 1% above or below the normalized point. Reliable contours cannot be drawn more than about 65^o from the central meridian because of foreshortening effects. Activity centers appear as "hot spots" (hills on the contour maps) with typical peak enhancements of 4% to 10%. Additionally, temperature slopes are calculated in the operationally simple units of percent enhancement per heliographic degree, and are typically a couple to a few tenths in these units, which we abbreviate as $\% \, (H^o)^{-1}$.

These two observational quantities are important because Mayfield et al. (1970) have shown that reliable forecasts of solar flares can be extracted from them. Specifically, they have shown that flares of optical class ≥2F can be expected to occur within 24 hrs (usually, or up to 48 hrs in some cases) after an active region attains a peak enhancement ≥8.5% and a temperature slope $\geq 0.5\% \, (H^o)^{-1}$. The present effort is directed toward extending the forecast capability to less intense flares, namely of classes 1N and 1B.

The criteria established as a result of the previous work were operationally useful; measurements could be made and class 2 flares could be anticipated or not anticipated on the basis of the measurements. The results at that time, though, fell short of providing all the physical insight one would desire to obtain about the active plage regions being measured. For example, the physical significance of the measured temperature slopes was not entirely understood; some of the hottest regions exhibited some of the steepest slopes, but what characteristics of the local sources on the sun would determine what slopes would be measured? This problem was re-addressed at the outset of the current effort to gain the understanding required to ensure the validity of any eventual forecasting method developed.

By inspection of numerous radio contour maps, it was noted that many enhanced regions appeared as nearly circular concentric contour lines, especially when any one region was relatively unconfused by other regions. This realization was taken as a hint that such regions were not being spatially resolved by the radio telescope. A brief explanation of this reasoning is appropriate here. One should begin by recalling that a transmitting antenna and a receiving antenna (like a radio telescope) can be understood in reciprocal terms, that is, in some respects one operates just "inverse" to the other. It is commonly understood that a transmitting antenna beams its signal preferentially in certain directions. Furthermore, because of the reciprocal relationship of receiving and transmitting antennas, a receiving antenna preferentially receives signals from certain directions. An example of these operational characteristics of a receiving antenna is familiar to anyone who has spent hours on a rooftop pointing a TV antenna in different directions to receive the best picture he can. He is demonstrating to himself the beamed response of his TV antenna.

In the case of the Aerospace 15-ft radio telescope, most of the signal received by the antenna must lie within a narrow cone around the pointing axis. The angular width of this cone is 2.8 arc min (HPBW). If one pointed the telescope directly at a point-source (no resolvable dimensions) so that the source lies exactly along an extension of the pointing axis, and took a measurement he would get a value M, which is the maximum value (peak response) one could obtain for this source with this telescope. (This corresponds to the "best" picture one could obtain on his TV set.) If the telescope is mispointed just slightly (or the TV antenna turned), the measured value of the source would be something less than M (the TV picture would degrade somewhat). The decrease in the measured signal from the point source is not due to the source or its shape (it is pointlike and shape can't be discerned) but only to the decreased response of the telescope antenna. How the response varies around the pointing axis is known as the beam shape; for the Aerospace telescope, the shape is very nearly Gaussian (bell-shaped). Hence, measurements of a point-source with the radio telescope would result in a peak measurement when the antenna points directly at the source and lower values as the antenna beam is moved around so that a lower response part of the beam is pointed directly at the source. If we make a contour map of these measurements, we would obtain concentric circular contours spaced appropriately for a bell-shaped "hill." In other words, the steepness of the slope down the "hill" would just be that appropriate to the beam shape. We would not have measured anything about the characteristics of the point-source except its peak response.

The point-source approximation is valid for a source not any larger than perhaps a fifth of a beamwidth. For larger sources, some of the shape and size will begin to be measured, but reliable shapes and sizes can only be determined for sources which are larger than the beamwidth (2.8 arc min). Both of these cases probably occur with active sunspot-plage regions on the sun, but we now realize that it is important to know whether or not we are resolving or, at least, partially resolving local sources on the sun so that we can know if the measured temperature slopes pertain to the solar regions or are merely characteristic of the antenna beam. With this distinction in mind, a plot of a region's peak temperature enhancement vs.

its average temperature slope in the direction of steepest descent is presented in Figure 1. The data here have been obtained from plage regions which appeared on contour maps from 13 February to 27 May 1971. The procedure for determining the peak enhancements emphasizes care in choosing the normalization point by restricting the choice to the central region ($\pm 35^{\circ}$ in longitude) of the disk and, with the aid of H α pictures, by eliminating regions with dark filaments visible or a history of dark filaments. Such regions can result in anomalously low normalization readings (see Kundu, 1970, and White, 1972, for a discussion) and, hence, anomalously high readings at other points on the disk. This caution has been maintained throughout the data analyzed in this report and, although such a procedure differs from that of earlier work (e.g., Mayfield et al., 1970), it should ensure a greater degree of homogeneity in the data. Likewise, a slightly different procedure for determining the average temperature slope in the direction of steepest descent has been employed: the measurement is made over a distance equal to 100 arc sec in the sky (the separation of data points on a map), so that the average pertains equivalently to a distance on the sun of six heliographic degrees near the center of the disk.

With these explanations clear, the meaning of the plot in Figure 1 can be interpreted. The points scatter above and to the left of the line indicating the temperature slope which the antenna would measure for a given peak temperature enhancement when a point source (completely unresolved source) is observed. This line is, therefore, just a "reflection" of the shape of the antenna beam. Observations of point sources (with no errors) would fall exactly along this line. When we view the antenna beam as a probe and realize that it has a finite width, then we see that we cannot hope to measure any radio sources narrower or more peaked than the limit imposed by the antenna beam. The final result, the response of the antenna, is always going to be as broad as the antenna beam plus the additional breadth of the radio source. This additional breadth for a given peak temperature enhancement means that the contour "hill" is "fatter" and, hence, the temperature slope is less; data points will scatter to the left, the further to the left indicating a larger and larger radio source on the sun.

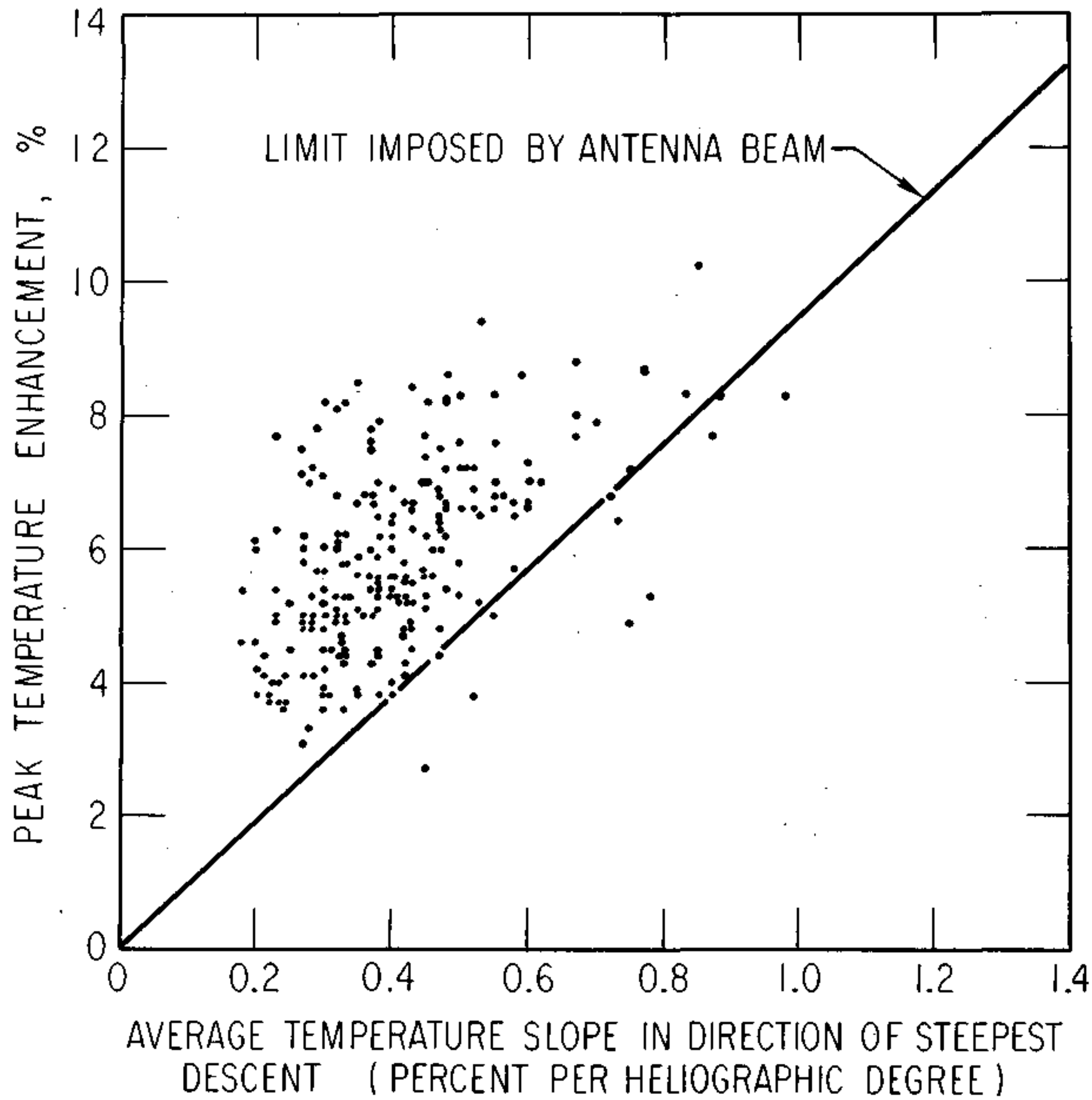

Figure 1. Peak temperature enhancement of plage regions from 13 February to 27 May 1971 vs the corresponding average temperature slope in the direction of steepest descent to a distance of 100 arc sec from the peak. The line indicates the theoretical demarcation imposed by the antenna beamwidth.

Not all the scatter in Figure 1 is real, of course. Some of the scatter is "noise" in the measurements due to clouds and jiggling of the antenna. Certainly, the points which fall below the line are physically impossible (the response of the antenna cannot be narrower than the antenna beam) and perhaps the only plausible explanation is that the background, undisturbed solar surface, is not even; for example, dark filaments threading through active regions could cause this type of result. Furthermore, the plot contains data from many different plage regions and they will, of course, exhibit a variety of sizes and any one radio plage region may vary in size from day to day. Future work is designed to unravel the contributions to the measured size due to the antenna beam and that actually attributable to the radio plage or radio sunspot; these contributions are still lumped together in Figure 1. The conclusion to be drawn from the plot which has a bearing on the present work is that the majority of data points lie close enough to the limiting line that most of the local radio sources will not be resolvable and that, therefore, the measurement of a region's average temperature slope is redundant information; one need only obtain a region's peak temperature enhancement to extract all the information one can regarding the intensity of the radio plage.

Before we can employ the peak temperature enhancement as a parameter correctly describing the local radio sources with complete confidence, we should test to determine whether there are foreshortening effects, due to the location of regions near the sun's limb, which would systematically alter our measurement of the true peak enhancements. This test has been performed in the plots in Figures 2 and 3. Measurements of the peak enhancements of the plage regions plotted in Figure 1 were made at different distances from the central meridian as the sun's rotation carried the regions across the solar disk. All the measurements of a single region were normalized to the maximum peak enhancement for that region, and then all such normalized peak enhancements for all the regions were plotted against their central meridian distances. The tremendous scatter in Figure 2 prevented any conclusions from being drawn, so Figure 3 was constructed from the 10°-averages of the data in Figure 2. Out to a distance of 30° any variation

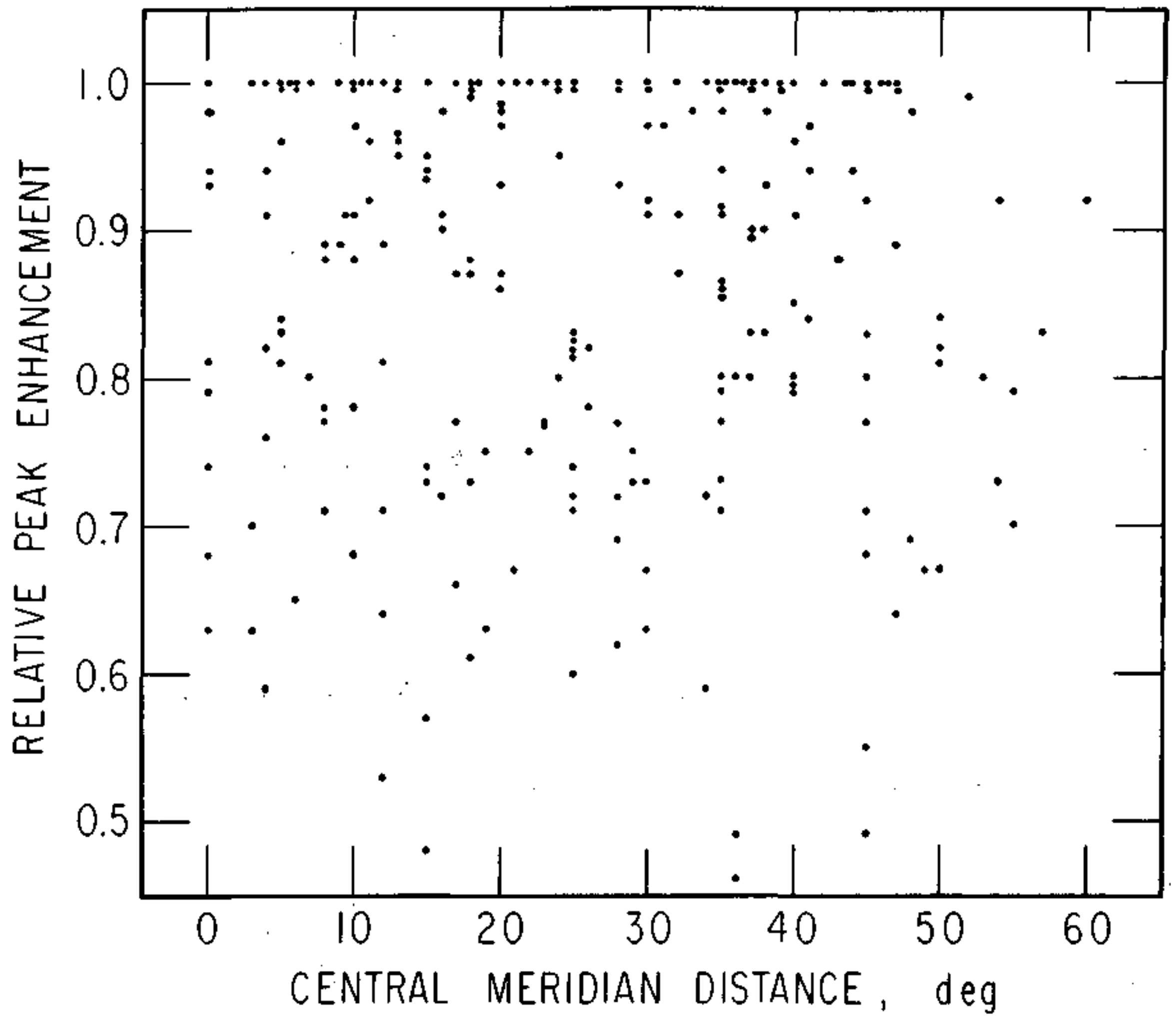

Figure 2. For the period 13 February to 27 May 1971, all the peak enhancements measured for a given plage region were normalized to the maximum such measurement for that plage region, and then all the relative peaks were plotted according to the central meridian distance of the peak.

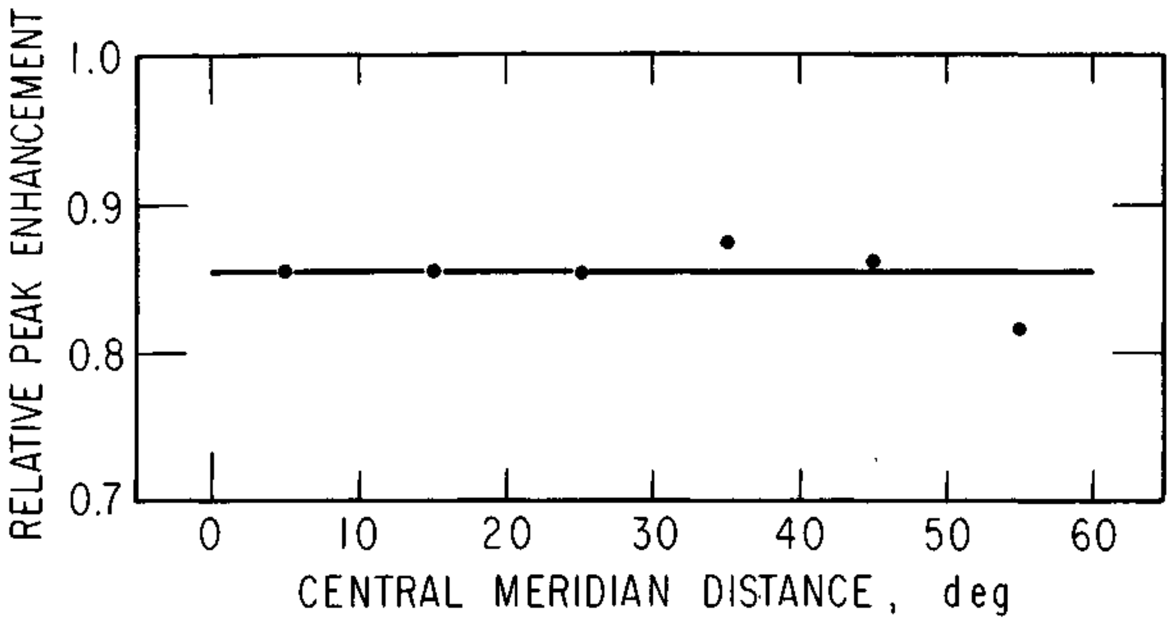

Figure 3. The tremendous scatter of Figure 2 is smoothed by forming 10° - averages of the data plotted in Figure 2. Out to 50°, the sample sizes are comparable and the scatter from a horizontal line is insignificant. The data point from 50° - 60° is low due to real effects, due to a small sample size, or a combination of both.

B

is remarkably absent; even the small variations out to 50° are considered insignificant. The fall-off from 50°-60° is at least partially due to a small sample size. We can conclude, based on the interpretations of Figures 1 and 3, that we will not be losing information about the radio plage regions by measuring only their peak temperature enhancements, and that we can rely on these measurements to be valid out to a distance of 50° for sure, and probably even 60°.

With these modifications to previous measurement techniques explained, we can proceed to a review of the data obtained.

II. REVIEW OF THE DATA

Since our purpose is to test the feasibility of forecasting class 1 solar flares on the basis of interpretation of 3.3-mm radio contour maps, the data necessary for the analysis logically fall into two categories: 1) data pertaining to solar flares that have occurred; and, 2) data extracted from the contour maps. The solar flare data are summarized in the flare-record chart of Figure 4. The information contained in this chart covers the period of 1 June 1970 to 30 June 1972 and includes all McMath plage regions which crossed the central meridian of the sun during that interval and produced at least one flare of optical class ≥ 1B (e.g. 1B, 2F, 2N, 2B, etc.). The calendar format of the chart is arranged on a 27-day rotation period of the sun and coincides with the Bartels rotations whose numbers appear at the extreme right-hand side. Each plage region qualifying to be on the chart is indicated with an open triangle whose vertex indicates the day and decimal of a day that the region crossed the central meridian. Northern regions are presented in the upper half of each 27-day row by triangles pointing down, while southern region triangles point up from below. The annotation on the left side of each triangle is the McMath plage number (the first one is #10780, the last is #11926), while on the right side is the latitude of the plage center. The data for each plage have been extracted from Solar Geophysical Data (Comprehensive Reports) for all plages through December 1971. Additionally, for all plages from August, 1970, through October, 1971, the regional flare index as computed by NOAA is included within the plage's triangle; the larger the number, the more flare activity the plage region exhibited. The data for January through March, 1972, have been extracted from Solar-Geophysical Data (Prompt Reports), while those for April, May, and June, 1972, come from Solar-Geophysical Data (Preliminary Reports), and the astericks indicate that the positions of the triangles are based on flare locations instead of plage locations.

The essence of the flare-record chart is the clustering of flare-productive plages along trend lines, which have been drawn in. When a plage has been identified as belonging to a recurrent family of flare-productive regions, the vertex has been blackened. The explanation for the recurrance of these regions is not yet clear, although some of the work by Sawyer (1968) may be related. In the present work we will find that plage regions which

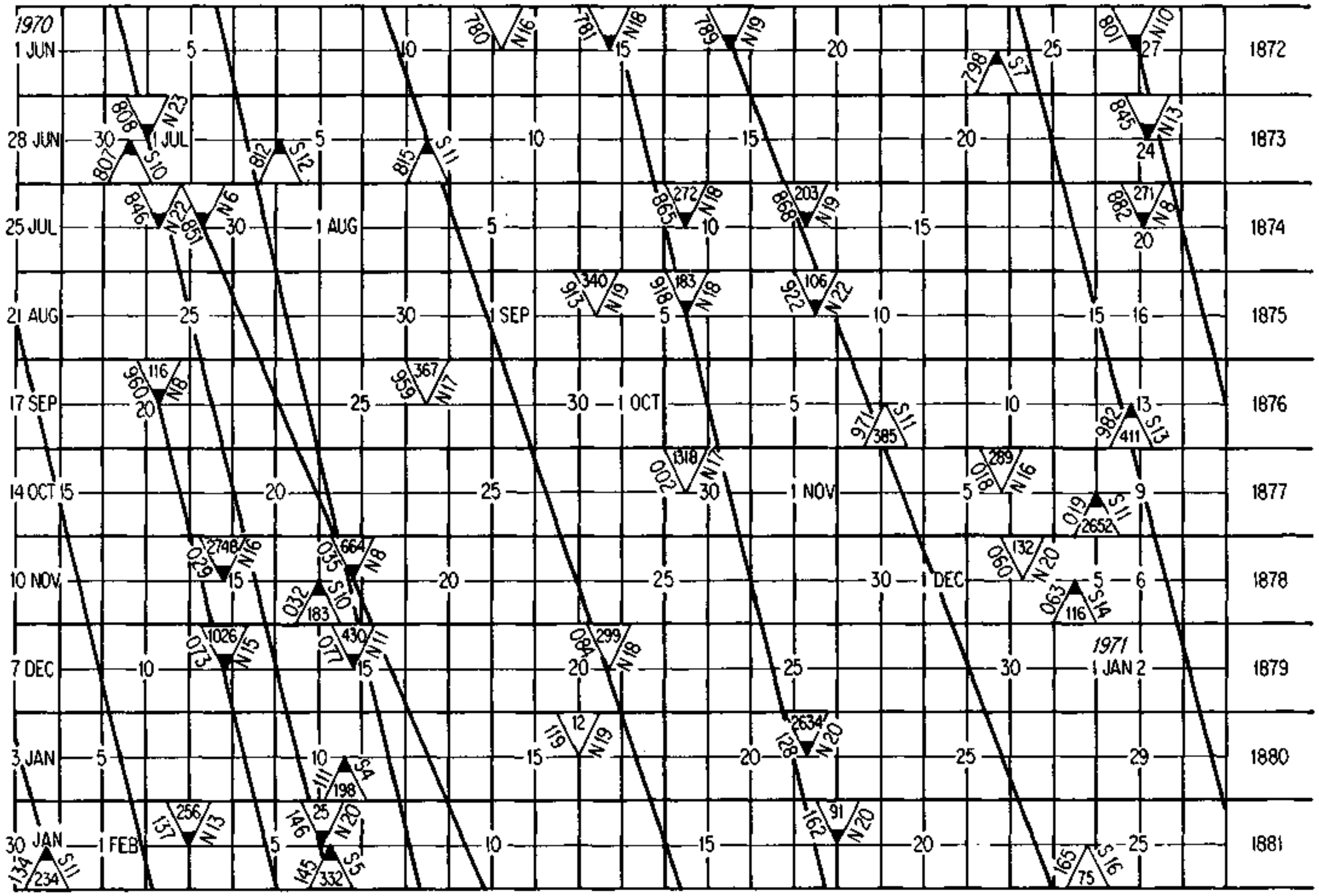

Figure 4. Flare-record chart covering the period 1 June 1970 to 30 June 1972. All plage regions producing flares of class ≥ 1B qualify to be on the chart and are represented by the triangle symbols, whose vertices indicate the day and decimal of a day of central meridian crossing. The McMath plage numbers from 10780 to 11926 are indicated, as well as the latitudes of the plage centers and the NOAA regional flare indices (inside the triangles). The plage regions identified as belonging to a recurrent family of flare-prone regions are indicated by blackened vertices.

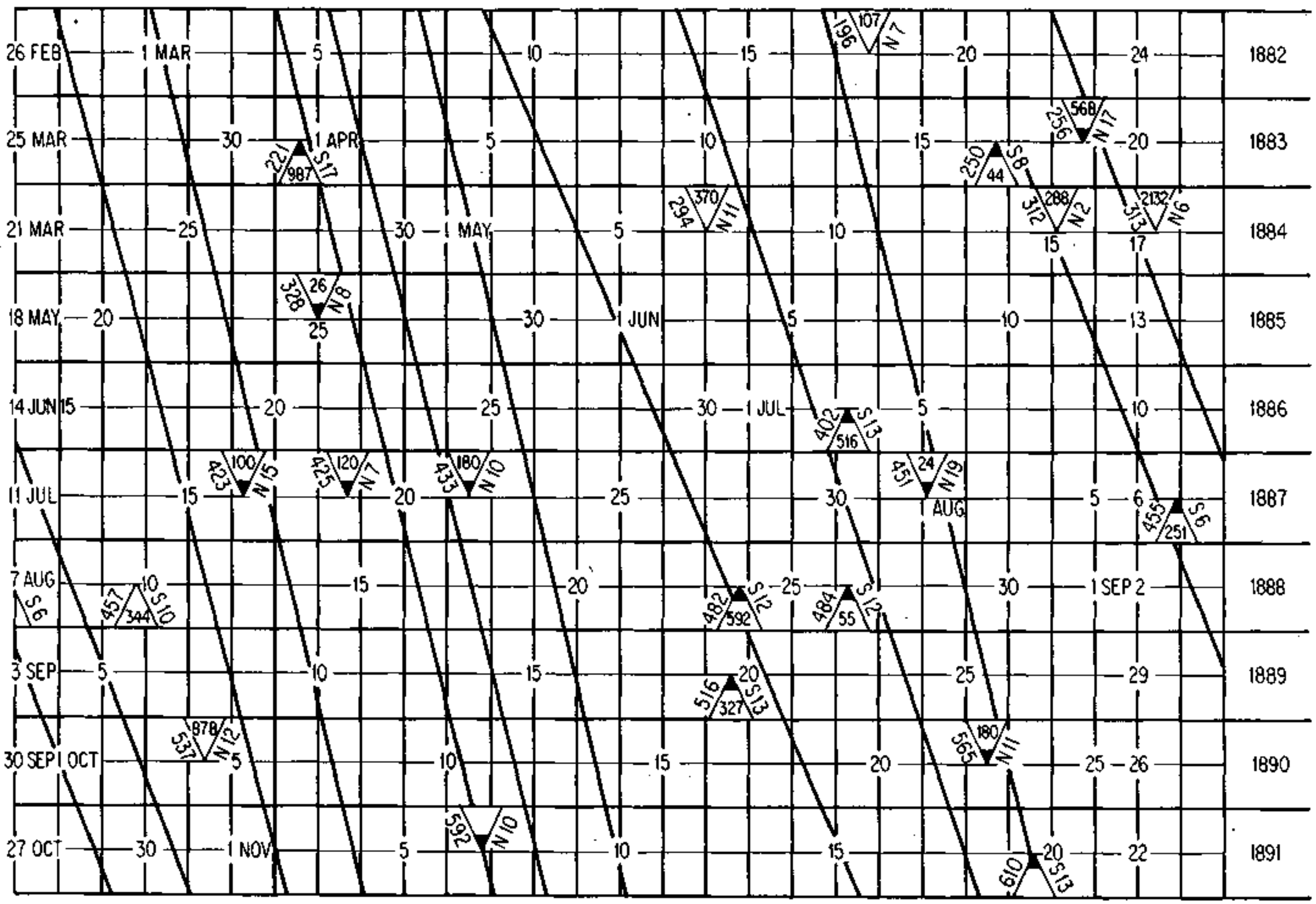

Figure 4. Continued

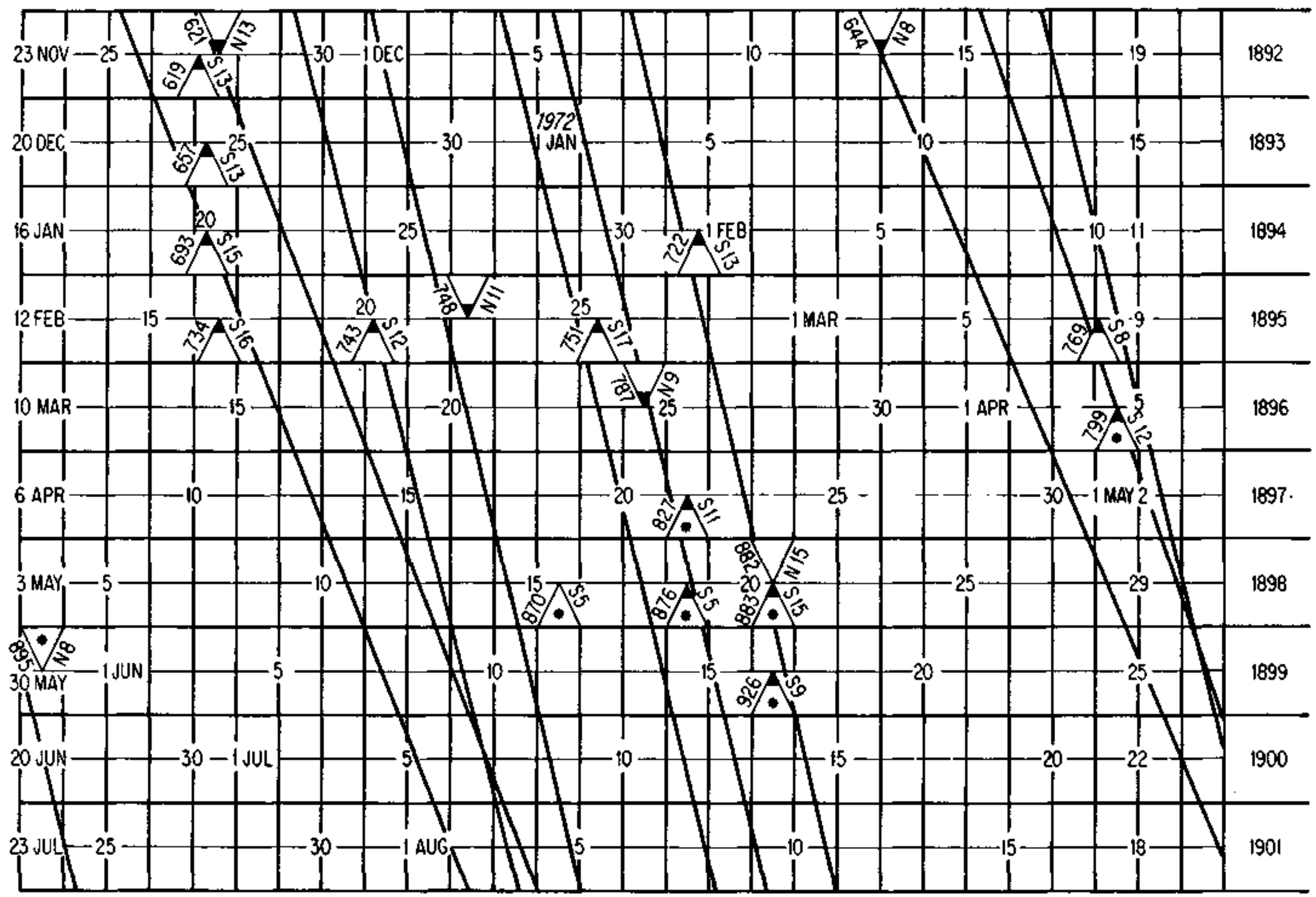

Figure 4. Continued

adhere to the trend lines differ from other plage regions in their 3.3-mm peak temperature enhancements and subsequent flare intensities.

Data were extracted from all the 3.3-mm contour maps for the period 1 July 1971 to 30 June 1972. For each plage region appearing on the contour maps, a peak temperature enhancement is obtained and plotted each day. Then, for any one plage, all the points observed during the passage of the plage across the disk are connected by straight lines. These plage "temperature histories" are presented in Figures 5 through 8, segregated according to the flares produced by the region. Furthermore, each day a flare occurred, a cross has been placed on the date of the flare at the peak temperature enhancement indicated for that region on the most recent previous map. For example, Figure 5 exhibits all plage regions producing class 2F, 2N, or 2B flares; region #11484 (written as 484) produced a class 2N flare on 27 August and the 3.3-mm peak enhancement was 5.0% on 26 August, rising to 6.9% on the map made on 27 August, but after the flare. Figure 6 exhibits all plage regions producing class 1B flares; region #11516 produced a 1B flare on 17 September after a peak reading of 10.0% on the previous day, with the next peak reading of 8.8% not being made until 18 September. Region #11516 also appears on Figure 7 because it produced a class 1N flare on 15 September. Sometimes a cross will appear in the same position on two different figures, because flares of more than one class occurred during that day. For example, region #11693 shows class 1B and 1N flares on 19 January (Figures 6 and 7, respectively), while the region also appears on Figure 5 due to a class 2B flare on 14 January. The data exhibited in Figure 8 pertain to plage regions which did not produce any reported flares classified as 1N or greater and, thus, no crosses appear on this figure. It should be noted that, while Figures 5, 6, and 7 contain complete samples (no qualifying plage regions fail to show up), Figure 8 has an incomplete sample, since many regions not producing flares never attained a minimum peak temperature enhancement to be reliably detected.

All the data available for the study encompassing FY 1972 are contained in Figures 4 through 8 plus a list of all flares of class $\geq$ 1N (a total of 152), which is not presented per se. What remains now is the analysis of these data to investigate the possibility of forecasting class 1 flares.

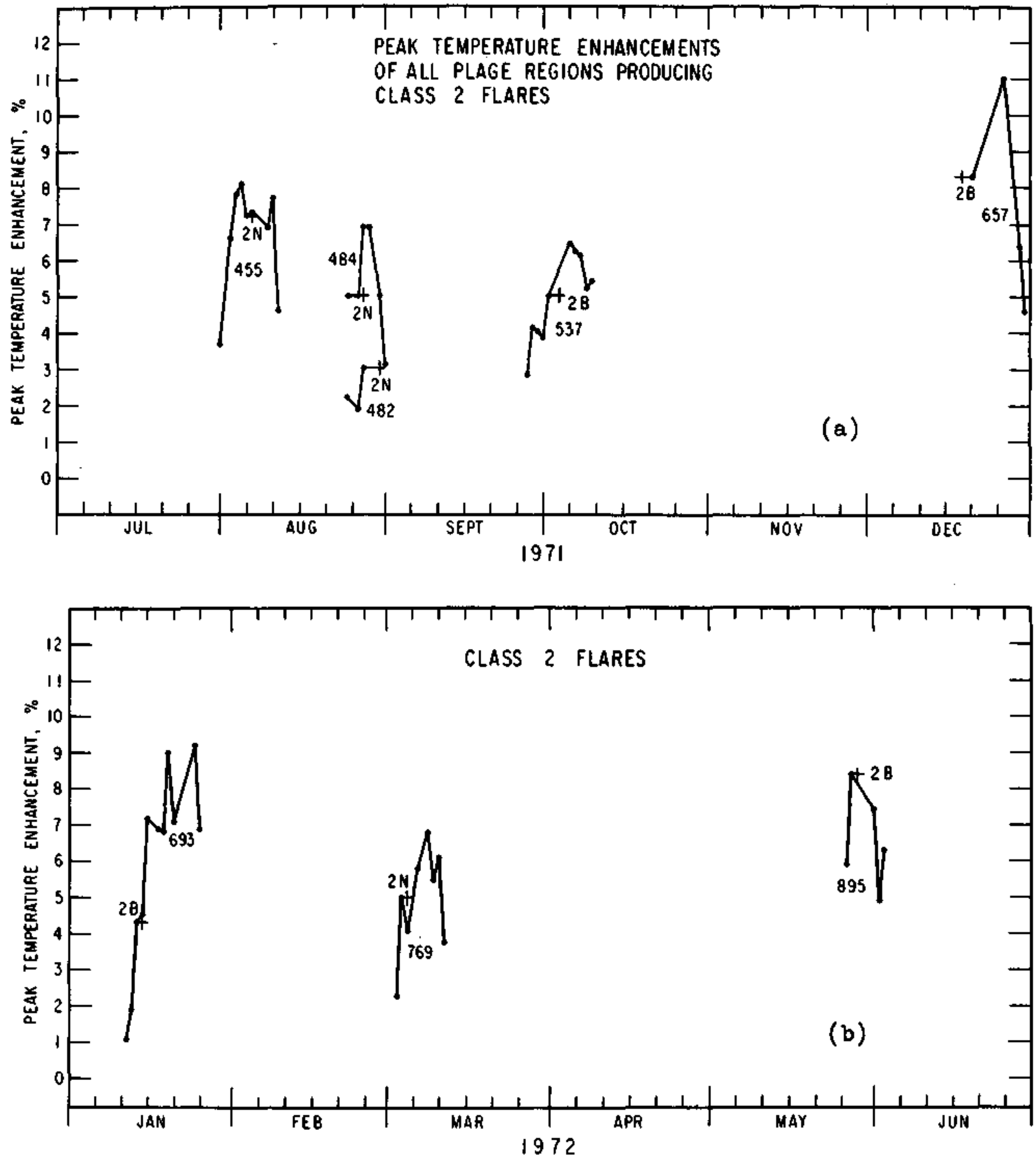

Figure 5. Peak temperature enhancement histories for all plage regions producing class 2 flares in FY 72. The crosses indicate the flare date and most recent pre-flare peak enhancement measurement. a. Data for 1 July through 31 December 1971; b. Data for 1 January through 30 June 1972.

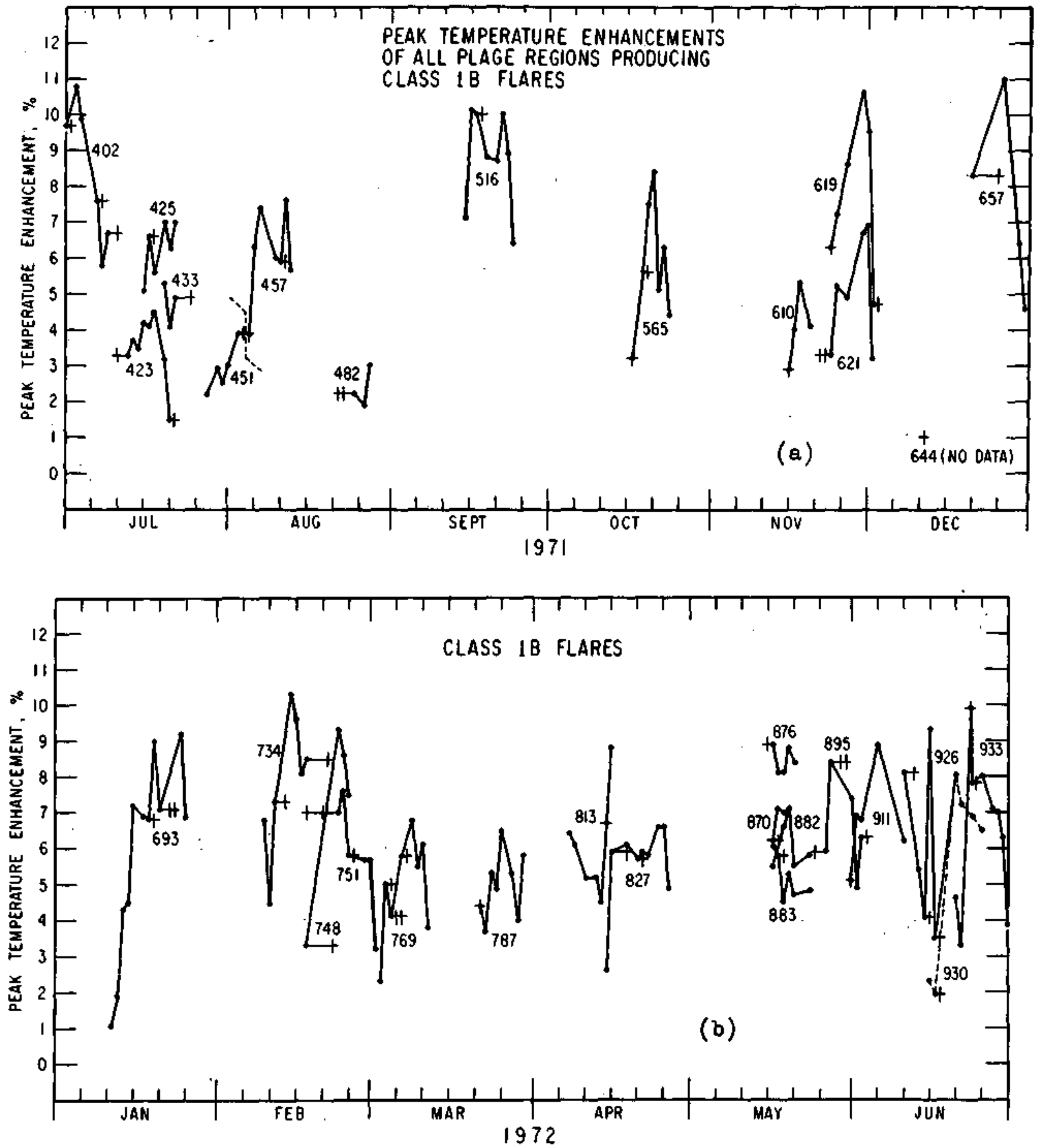

Figure 6. Peak temperature enhancement histories for all plage regions producing class 1B flares in FY 72. The crosses indicate the flare date and most recent pre-flare peak enhancement measurement. a. Data for 1 July through 31 December 1971; b. Data for 1 January through 30 June 1972.

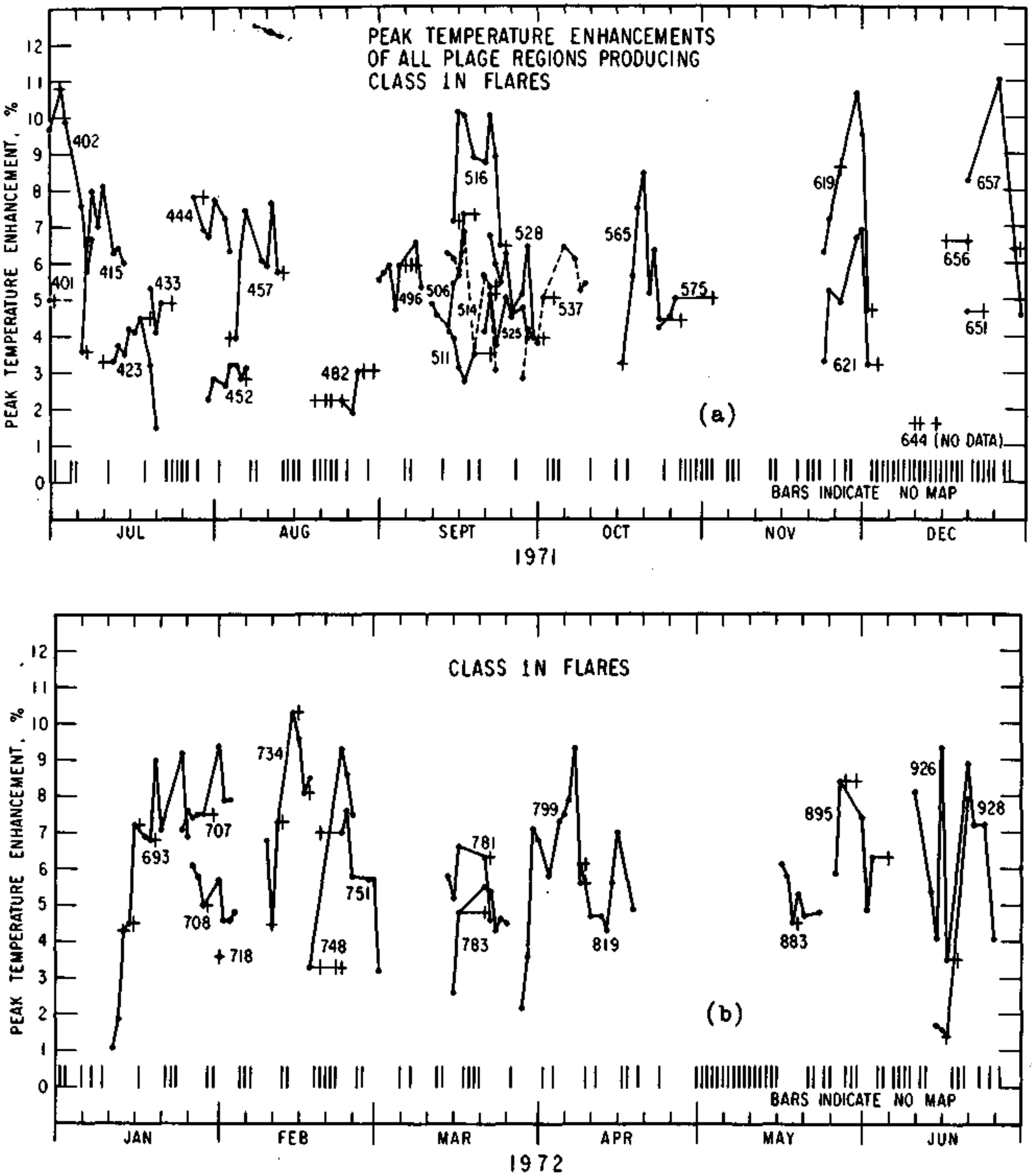

Figure 7. Peak temperature enhancement histories for all plage regions producing class 1N flares in FY 72. The crosses indicate the flare date and most recent pre-flare peak enhancement measurement. a. Data for 1 July through 31 December 1971; b. Data for 1 January through 30 June 1972.

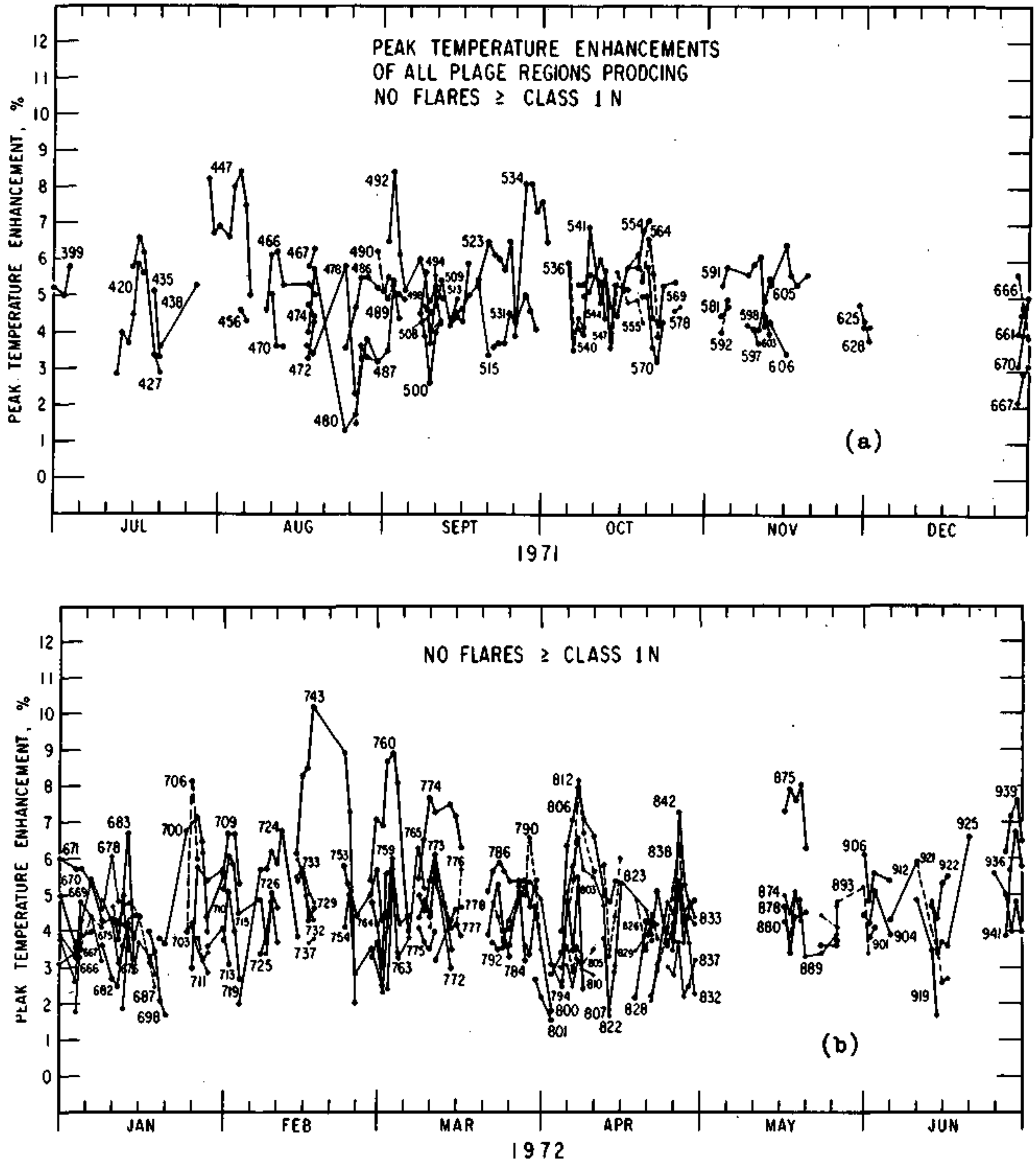

Figure 8. Peak temperature enhancement histories for all plage regions producing no flares ≥ class 1N in FY 72. The crosses indicate the flare date and most recent pre-flare peak enhancement measurement. a. Data for 1 July through 31 December 1971; b. Data for 1 January through 30 June 1972.

III. ANALYSIS OF THE DATA

Without any further preparation or sifting of the data in Figures 5 through 8, attempts were made to understand the relationship between preceding 3.3-mm peak temperature enhancements and flare occurrence and flare class by means of various averages of regions which produced a certain class of flare. For example, the average pre-flare 3.3-mm peak enhancement was computed for all regions which eventually produced class 1B flares. Other averages included the average peak enhancement measured just following a flare event and the average net change in enhancement from measurements before and after the flare. Differences in the averages, of course, existed, and one could interpret the results in a way which made sense. It was felt, though, that the data were being compromised, that more definitive statements about the probability of flare occurrence could be made. To do this required some refinement of the data sample. The following discussion explains the logic behind those refinements.

Contours on the radio maps can be drawn and read accurately to a distance of about 65° from the central meridian. Beyond this limit foreshortening due to proximity to the limb becomes so great that the contours are squeezed too close together for accurate measurement. Furthermore, the data presented in Figure 3 indicate that the peak temperature enhancements measured between 50°-60° from the central meridian may be slightly reduced from their true values, perhaps also due to foreshortening or some sort of anisotropy in the radio sources. The apparent decrease may also be due to a statistical fluctuation due to the small sample size in that interval. In light of these considerations, measurements of peak temperature enhancements made beyond 60° were deleted from further analysis.

It was noticed in Figure 8 that the majority of regions not producing any flares $\geq$ 1N clustered around a peak enhancement of about 5% with a spread from day to day of perhaps $\pm$ 1%, some of which is noise and some of which is evolution of the regions. (This mean is below the mean peak enhancements measured before class 1N and 1B flares, which were 6.2% and 6.4%, respectively.) Standing out above the crowd in Figure 8, though, are a number of regions that reached a maximum peak enhancement in excess of 8% without flaring. These regions were examined as a group and were found to be almost exclusively plage regions which did not lie along the flare trend lines in Figure 4 and they are, therefore, called virgin regions, since they have ho history of flare activity according to the flare-record chart. Regions which do lie along the trend lines, even those which do not produce flares during a given disk passage, are said to have positive flare histories. The data of Figures 5-8 were then re-examined with a division into these two categories.

Table I presents data for plage regions with positive flare histories in an analysis designed to investigate plage regions prior to class 1B flares. All the data in Table I are the reliable data selected from Figure 6 for regions which did produce class 1B flares plus the reliable data from Figure 7 for regions which produced 1N flares, but not any greater, and from Figure 8. All the entries are ranked in descending order. The entries from Figure 6 are the pre-flare peak temperature enhancements, while the entries from Figures 7 and 8 are the maximum peak temperature enhancements attained by the non-flaring plage regions. Additionally, there are forty-six plage regions with positive flare histories (but no 1B flares) which were below the threshhold of reliable detection on the contour maps, and they, supposedly, would all be ranked near or below the 3.4% maximum peak of plage #11667. By inspection of Table I, one sees that the flaring plages are generally concentrated near the head of the list and, in fact, the hottest three regions all produced class 1B flares. Furthermore, near the bottom of the list there is a depletion of the regions which did not flare because of the threshhold for detectability, as mentioned above.

The data of Table I were analyzed by grouping the data together over a span of 0.5% and calculating the percentage of the group which produced 1B flares. The resulting data points are plotted in Figure 9 and fit with an eyeballed best-fit curve. The first three data points from 3-4.5% have not been included in the fit because of the depleted sample of non-flaring regions, as explained above, which would incorrectly boost the plotted points. Also, the seven data points above 7.8% are excessively scattered because of the thinly distributed temperature enhancements ranked near the hot end, and they have been excluded from the curve fitting. Finally, it will be noted that the sample indicates that all positive flare history plage regions with peak enhancements $\geq 9.7\%$ will produce class 1B flares.

Table I. Regions with positive flare histories: class 1B flares

Plage #	Max. Peak % (No Flares >1N)	Pre-Flare Peak, % (1B Flares)	Plage #	Max. Peak % (No Flares >1N)	Pre-Flare Peak, % (1B Flares)	Plage #	Max. Peak % (No Flares >1N)	Pre-Flare Peak, % (1B Flares)
11516		10.0	540	5.9		698	4.0	
933		9.9	883		5.8	451		3.9
402		9.7	751		5.8	711	3.8	
707	9.4		769		5.8	721	3.7	
799	9.3		569	5.8		543	3.6	
928	8.9		827		5.7	926		3.5
895		8.4	565		5.6	667	3.4	
415	8.1		498	5.6				
534	8.1		783	5.5				
933		7.8	792	5.4				
444	7.8		823	5.4				
402		7.6	515	5.3				
734		7.3	435	5.1				
506	7.3		828	5.1				
842	7.3		570	5.0				
693		7.1	661	5.0				
819	7.0		670	5.0				
541	6.9		754	5.0				
693		6.8	542	4.9				
724	6.8		592	4.9				
813		6.7	676	4.8				
528	6.7		687	4.8				
709	6.7		619		4.7			
425		6.6	568	4.7				
781	6.6		581	4.7				
523	6.5		778	4.7				
895		6.3	456	4.6				
765	6.3		580	4.4				
467	6.3		606	4.3				
490	6.2		628	4.3				
591	6.1		686	4.3				
671	6.0		703	4.2				
509	5.9		926		4.1			
536	5.9		769		4.1			

plus 46 regions, with no flares >1N, which were below the thresh-hold of reliable detection

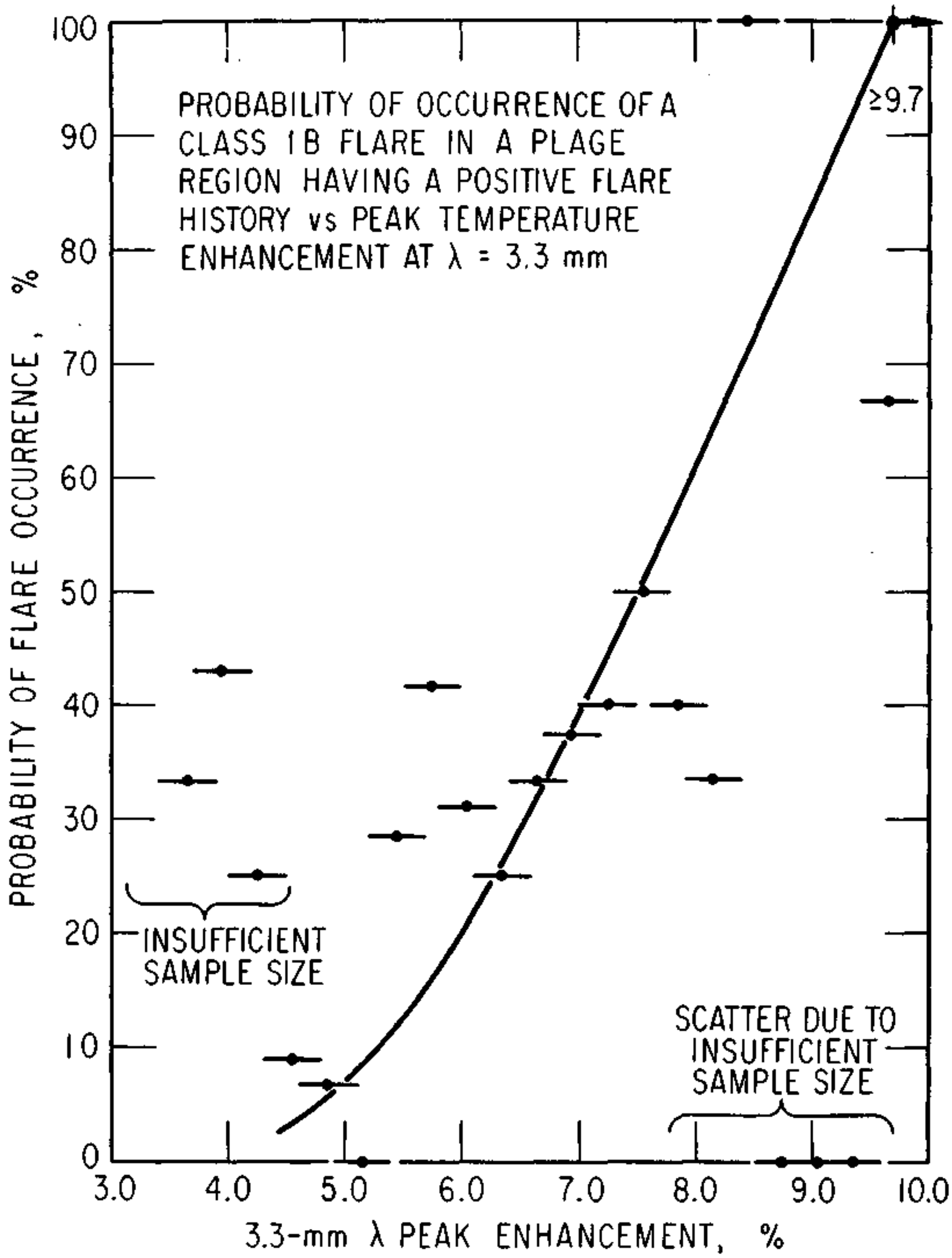

Figure 9. Data taken from Table I (averaged over 0.5% ranges) showing the probability of occurrence of a class 1B flare during a flare-prone plage region's disk transit as a function of the daily measured peak temperature enhancement. See text for discussion of the non-fitted data points.

Table II is a repeat in format of Table I, but now the data pertain to plage regions with positive flare histories which did produce a class 1N flare, but not greater (from Figure 7), and those which produced no flares at all (from Figure 8). The same comments about the depletion of the sample of non-flare regions ranked near the bottom of the list apply to Table II as they did to Table I and, consequently, the data points from 3-4.6% plotted in Figure 10 have been excluded from the curve fitting procedure. Once again, in Figure 10, the plotted points represent averages over a span of 0.5 % in temperature enhancement. For example, the average probability of occurrence of a 1N flare when the peak enhancement lies between 6.4% and 6.9%, inclusive, is 33% as found from the data in Table II and plotted in Figure 10. Unlike the data for the 1B flares, the data for the 1N flares are distributed more evenly toward the 100% probability level (at 8.4% enhancement), which makes it unnecessary to discard any of the higher peak enhancement data points from Figure 10. Based on the data sample, all positive flare history plage regions with peak enhancements ≥ 8.4% will produce class 1N flares.

Nothing has been said about analysis of class 2 flares, because the sample sizes are so small. A qualitative discussion of these flares will be presented in the next section. Also, it does not make sense to analyze the class 1B flares which occurred in virgin plage regions (negative flare history), since there were only three examples, two of which had reliable pre-flare peak temperature measurements of 5.9% and 6.2%. On the other hand, the sample of class 1N flares from virgin regions, while not large, is worth analyzing. The data are presented in Table III. The distribution of flaring regions, as seen from the table, is vastly different from the other two groups analyzed; flares occurred in 9 of the 109 regions. Even this rate of occurrence is an inflated estimate of the true rate, since more than 300 other regions were assigned Mc Math plage numbers and did not flare, but their peak enhancements fell below the threshhold for reliable detection. Figure 11 exhibits the "inflated" data points taken from Table III. At best, the probability of occurrence of a class 1N flare in a virgin region never exceeds 10-20%. The scatter of data points for enhancements from 5-6% is not unlike those in Figures 9 and 10, but for some not understood reason the appearance of 1N

Table II. Regions with positive flare histories: class 1N flares

Plage #	Max. Peak, % (No Flares)	Pre-Flare Peak, % (1N Flares)	Plage #	Max. Peak, % (No Flares)	Pre-Flare Peak, % (1N Flares)
11402		10.8	828	5.1	
734		10.3	570	5.0	
619		8.6	661	5.0	
895		8.4	670	5.0	
734		8.1	754	5.0	
534	8.1		433		4.9
444		7.8	542	4.9	
707		7.5	592	4.9	
506		7.3	676	4.8	
842	7.3		687	4.8	
693		7.2	619		4.7
700	7.2		578	4.7	
516		7.1	581	4.7	
554	7.1		778	4.7	
541	6.9		456	4.6	
693		6.8	883		4.5
724	6.8		423		4.5
709	6.7		580	4.4	
523	6.5		606	4.3	
516		6.4	628	4.3	
781		6.3	686	4.3	
765	6.3		703	4.2	
467	6.3		698	4.0	
490	6.2		528		3.9
591	6.1		711	3.8	
671	6.0		721	3.7	
509	5.9		415		3.6
536	5.9		543	3.6	
540	5.9		926		3.5
569	5.8		667	3.4	
799		5.6	748		3.3
498	5.6		621		3.2
792	5.4		482		3.0
823	5.4				
515	5.3				
435	5.1				

plus 46 regions with no flares ≥1 N, which were below the threshhold of reliable detection

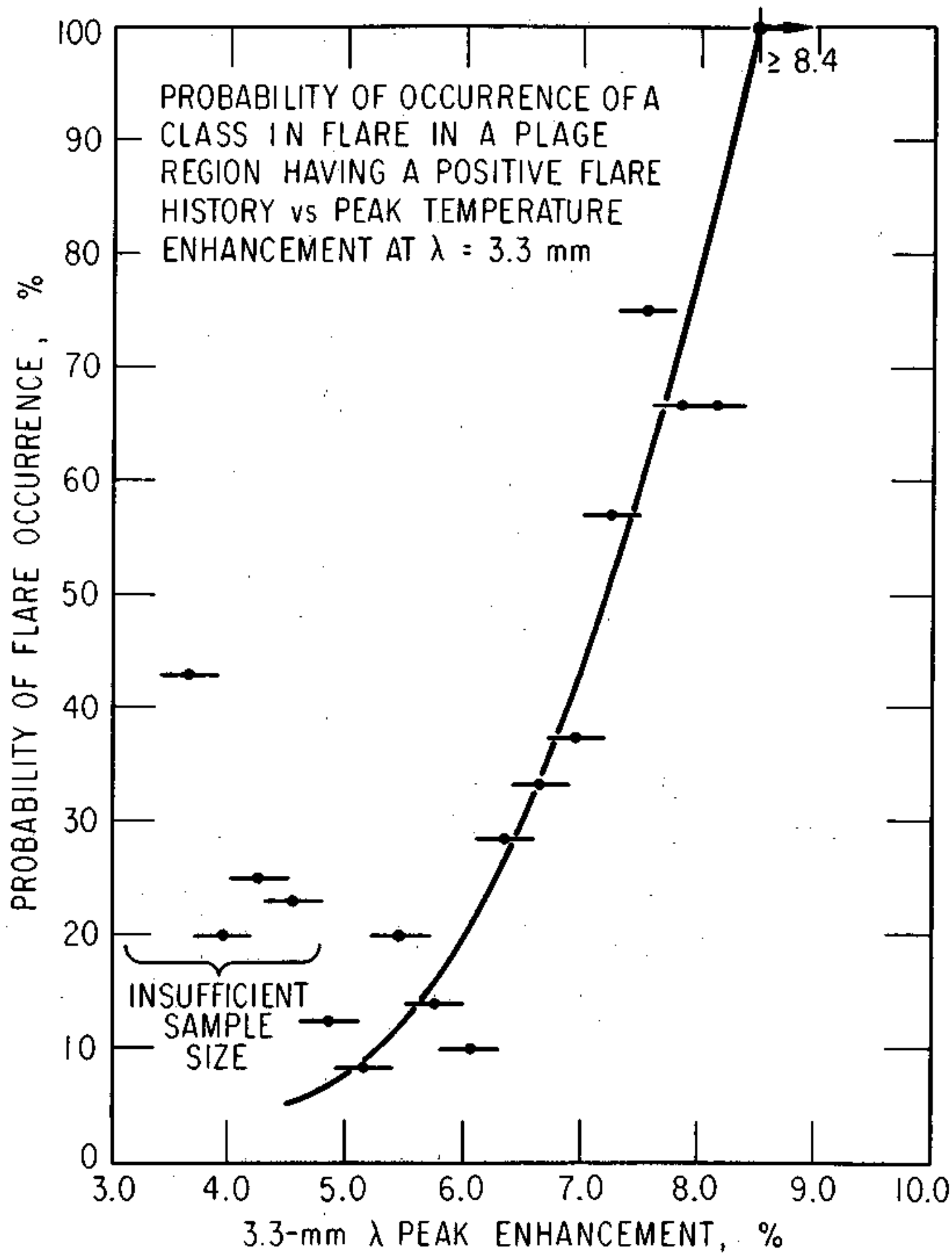

Figure 10. Data taken from Table II (averaged over 0.5% ranges) showing the probability of occurrence of a class 1N flare during a flare-prone plage region's disk transit as a function of the daily measured peak temperature enhancement. See text for discussion of non-fitted data points.

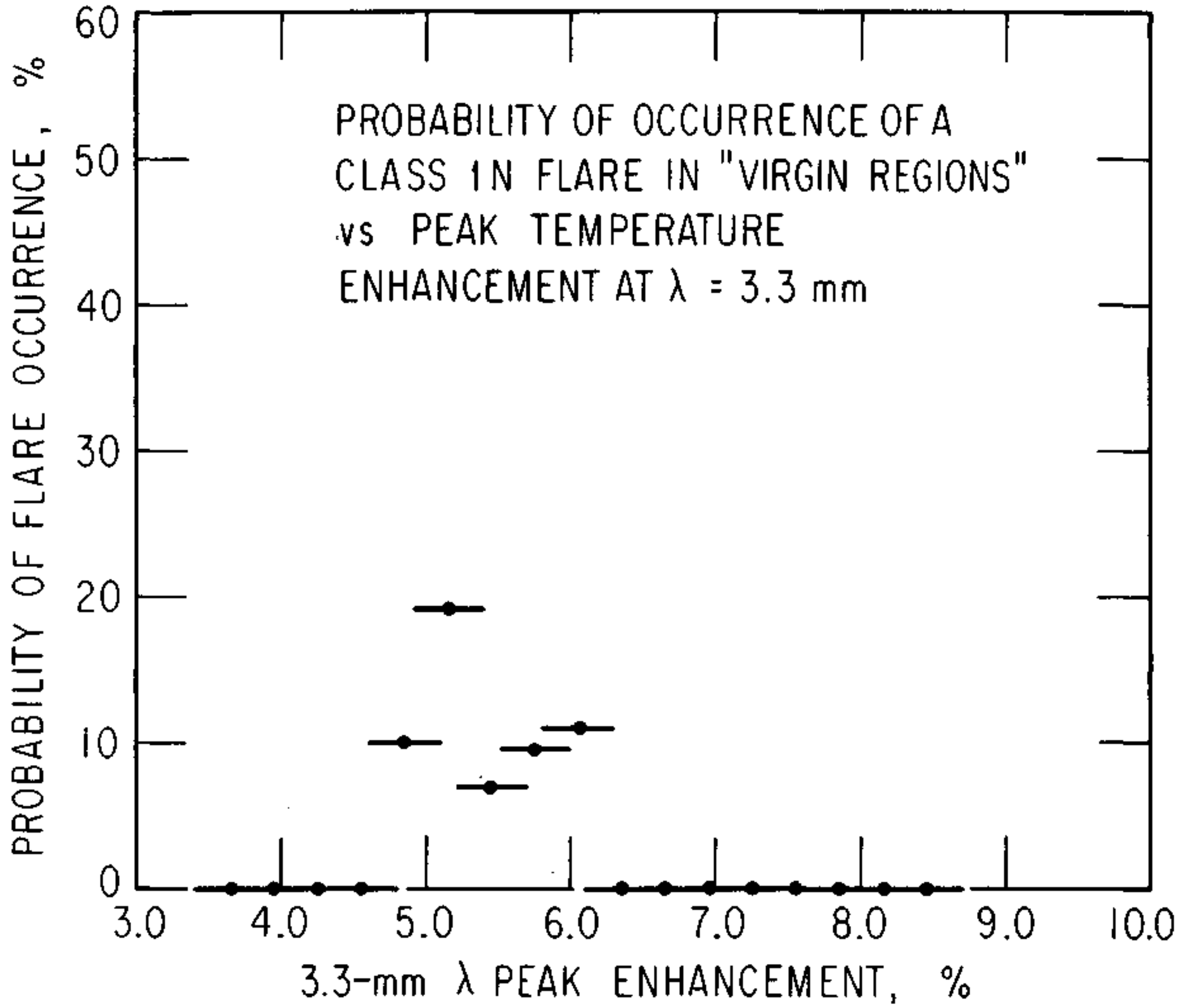

Figure 11. Data taken from Table III (averaged over 0.5% ranges) showing the probability of occurrence of a class 1N flare during a virgin plage region's disk transit as a function of the daily measured peak temperature enhancement.

Table III. Virgin regions: class 1N flares

Plage #	Max. Peak, % (No Flares)	Pre-Flare Peak, % (1N Flares)	Plage #	Max. Peak. % (No Flares)	Pre-Flare Peak, % (1N Flares)	Plage #	Max. Peak, % (No Flares)	Pre-Flare Peak, % (1N Flares)	Plage #	Max. Peak, % (No Flares)	Pre-Flare Peak, % (1N Flares)
12743	10.2		753	5.8		904	5.1		810	3.3	
760	8.9		871	5.8		537		5.0	840	3.2	
447	8.4		457		5.7	708		5.0	452		2.8
492	8.4		480	5.7		401		5.0	801	2.7	
812	8.2		555	5.7		470	5.0				
706	8.1		729	5.7		531	5.0				
806	8.0		764	5.7		832	5.0				
875	8.0		766	5.7		513	4.9				
774	7.7		772	5.7		826	4.9				
939	7.6		776	5.7		880	4.9				
683	6.7		544	5.6		919	4.9				
941	6.7		666	5.6		625	4.8				
427	6.6		710	5.6		725	4.8				
564	6.6		732	5.6		474	4.7				
790	6.6		763	5.6		508	4.7				
807	6.6		936	5.6		800	4.7				
925	6.6		486	5.5		878	4.7				
605	6.4		598	5.5		889	4.7				
838	6.4		803	5.5		603	4.5				
466	6.2		922	5.5		675	4.5				
678	6.1		669	5.4		682	4.4				
715	6.1		777	5.4		472	4.3				
773	6.1		794	5.4		500	4.3				
906	6.1		833	5.4		829	4.3				
547	6.0		514		5.3	597	4.2				
733	6.0		438	5.3		713	4.1				
759	6.0		489	5.3		775	4.1				
496		5.9	784	5.3		901	4.1				
496		5.9	835	5.3		737	3.8				
420	5.9		494	5.2		822	3.8				
786	5.9		893	5.2		837	3.7				
912	5.9		525		5.1	--	3.7				
921	5.9		719	5.1		487	3.6				
399	5.8		726	5.1		805	3.6				
478	5.8		874	5.1		796	3.3				

flares in hotter plage regions fails to occur. Furthermore, the flares which did occur were markedly deficient in the production of 1-8 Å x-rays; only one of the regions (#11496) produced a moderate flux of x-rays, while all the others produced minimal detectable levels or no detectable increase at all. The reasons for these characteristics are not understood, but it is clear that we have isolated a certain type of plage region unlikely to produce energetic flare activity, even when the peak temperature enhancements are high.

IV. INTERPRETATION OF THE RESULTS

The results of the study are effectively summarized by the plots in Figures 9, 10, and 11. The information contained in these plots can have very worthwhile application in providing forecasts of the probability that class 1B or 1N flares will occur in specific active plage regions. The explanation of how to prepare such forecasts follows directly.

The routine procedure begins with examination of the daily solar radio map made at the Aerospace Corporation. With reference to H α pictures, a normalization point is chosen in an undisturbed region and the peak temperature enhancements of various plage regions are accordingly calculated. For those regions of interest (perhaps with peak enhancements $\geq 5.0\%$), it is determined from the flare-record chart of Figure 4 which regions have positive flare histories. For the regions identified at this time as virgin regions, it is probably safe to discount any flare likelihood, regardless of the observed peak enhancement, on the basis of the data in Figure 11. On the other hand, for the regions with positive flare histories, one should refer to Figures 9 and 10. Let us suppose that a certain region exhibits a peak enhancement of 7.4%. Then from Figure 9 we can infer that there is a probability of 48% that this region will be the site of a class 1B flare during its disk transit. Likewise, from Figure 10 we infer that the region has a probability of 56% of producing a class 1N flare during its disk transit. Furthermore, if the peak enhancement the next day has risen to 8.1%, let us say, then the probabilities will be increased to 63% for 1B flares and 82% for 1N flares. The value of this ability to make definitive forecasts of flare probabilities is obvious to anyone desiring to optimize a flare observation program.

Some final comments need to be made about class 2 solar flares and the 3.3-mm observations preceding them. FY 72 witnessed a considerable decrease in the frequency of large, energetic solar flares, in accordance with the fact that solar cycle #20 reached its maximum in 1968-1969 and is now on the decline. Of the class 2B flares which occurred, only two had reliable pre-flare measurements made; namely, 5.0% two days prior to the flare and 8.4% one day prior to the flare. The first flare, which appears to be a legitimate, moderately energetic 2B, occurred in a virgin region which never attained a peak enhancement in excess of 6.4%. The second flare, plus two others with unreliable pre-flare measurements, were all produced in plage regions with positive flare histories; they reached maximum peak enhancements of 8.4%, 9.2%, and 11.0%. This final peak is the largest enhancement measured for any plage region during FY 72, so that even though statistically significant conclusions cannot be drawn regarding class 2B flares, the indications are that such flares occur more likely in "hotter" regions.

All four confirmed 2N flares occurred in regions with positive flare histories. Only three of these had reliable pre-flare measurements made and any conclusions will have to await a larger sample.

REFERENCES

Kundu, M. R.: 1970, Sol. Phys. 13, 348.

Mayfield, E. B., Higman, J. A., and Samson, C. F.: 1970, Sol. Phys. 13, 372.

Sawyer, C.: 1968, Ann. Rev. Astron. Astrophys. 6, 115.

Solar-Geophysical Data, U.S. Department of Commerce (Boulder, Colo.).

White, III, K. P.: 1972, "Temperature Depressions at $\lambda = 3.3$ mm", presented at SPD meeting of AAS at University of Maryland.

INTERNAL DISTRIBUTION

R. A. Becker
G. A. Chapman
E. N. Frazier
T. J. Janssens
D. J. Jensen
G. W. King
E. B. Mayfield
F. A. Morse
G. A. Paulikas

H. F. Prime
H. R. Rugge
F. Shimabukuro
T. Shiokari
J. H. Underwood
D. Vrabec
A. B. C. Walker, Jr.
E. T. Welmers
K. P. White, III